

Dark matter equation of state from rotational curves of galaxies

J. Barranco,^{1*} A. Bernal,^{2†} D. Núñez,^{3‡}

¹*Departamento de Física, División de Ciencias e Ingenierías, Campus León, Universidad de Guanajuato, León 37150, México.*

²*Área Académica de Matemáticas y Física, Universidad Autónoma del Estado de Hidalgo, Carretera Pachuca-Tulancingo Km. 4.5, C.P. 42184, Pachuca, Hidalgo, México.*

³*Instituto de Ciencias Nucleares, Universidad Nacional Autónoma de México, Circuito Exterior C.U., A.P. 70-543, México D.F. 04510, México.*

11 November 2018

ABSTRACT

In this work we model galactic halos describing the dark matter as a non zero pressure fluid and derive, not impose, a dark matter equation of state by using observational data of the rotation curves of galaxies. In order to reach hydrostatic equilibrium, as expected for the halo, it is mandatory that dark fluid's pressure should not be zero. The equation of state is obtained by solving the matter-geometry system of equations assuming different dark matter density or rotational velocity profiles. The resulting equations of state are, in general, different to a barotropic equation of state. The free parameters of the equation of state are fixed by fitting the observed rotational velocities of a set of galaxies.

Key words: Dark Matter fluid, pressure, equation of state.

1 INTRODUCTION

Astrophysical observations of the red shift of stars in galaxies, of the cosmic microwave background anisotropies, of the deflection of the light of distant galaxies, among others, are all explained by the presence of dark matter, which has not shown any interaction with the baryonic matter except the gravitational one. See Bertone (2005), Dodelson (2003) and Binney & Tremaine (2010), for a thorough discussion on dark matter.

On the other hand, direct detection of dark matter demands it to have some interaction with the rest of particles of the standard model, see Smith (1990) and Gaitskill (2004). These two research lines seem to have contradictory points of view on the properties of the dark matter. In order to attempt to conciliate these seemingly opposite strategies, one can research on the possibility that the astrophysical description of dark matter could relax the pressureless hypothesis, and allow some interaction with itself and/or with the baryonic matter.

For instance, at the cosmological level, Müller (2005) proposed a barotropic relation for the dark fluid, $p = \omega_{\text{DM}} \rho$, instead of considering the usual dust case ($\omega_{\text{DM}} = 0$). The author shows that the combined analysis of data from

anisotropies of the cosmic microwave background, supernovae Ia and matter power spectra constrain ω_{DM} to lay within the interval $[-1.5, 1.13] \times 10^{-6}$ (see also Calabrese et al. (2009), and also Avelino et al. (2012)), implying that a small, but non-zero dark matter pressure within the Λ CDM model, remains to be consistent with the observations. Furthermore, in order to avoid that intermediate mass black holes grow to values beyond the observed upper limits due to dark matter accretion, it seems mandatory that dark matter, modeled as a fluid, should have a non zero pressure, as pointed out in Pepe et al (2011). The same conclusion applies for Super massive black holes Guzman & Lora-Clavijo (2011). Note that the dark pressure is not likely to have an electromagnetic nature, so that it should have a different origin, raising as a kinetic pressure, for instance, or be of a weak interaction type.

Since one of the strongest evidence for dark matter comes from the rotational curves, it is natural to relax the pressureless hypothesis at galactic scales when describing the dark matter as a fluid. In the present work, we show that if dark matter is described by a perfect isotropic fluid, assuming a spherical symmetric and static space-time, a functional relation between pressure and energy density emerges using only the rotational velocity profiles. If the isotropic assumption is relaxed, then it is needed another observation to determine the equation of state. Such observation can be the gravitational lensing, see for instance Faber & Visser

* jbarranc@fisica.ugto.mx

† argelia_bernal@uaeh.edu.mx

‡ nunez@nuclares.unam.mx. Affiliated to IAC.

(2006), Núñez et al (2010), and Serra & Romero (2011) for a further discussion on the topic.

There are other works where both luminous and non-luminous matter is considered in axial symmetric space times with no pressure fluids, that is, models where the halo is rotating, see for instance (Cooperstock & Tieu 2005a; Cooperstock & Tieu 2005b; Cooperstock & Tieu 2006; Cooperstock & Tieu 2007; Cooperstock & Tieu 2008; Carrick & Cooperstock 2012)). It might be interesting to study in a future work those models and test the derivation of the equation of state for several halo models, as well as the Newtonian approximation in that case.

In order to show how to obtain the equation of state for the dark matter, we have organized the article as follows: In Section 2 we present the general relativistic equations for an isotropic perfect fluid in a spherically symmetric and static spacetime, and discuss how one of the metric coefficients is completely determined by the rotational curve profile. Hence, the resulting system of three equations involves three unknowns: the dark matter fluid pressure and density, and the other metric coefficient, that is, the system is closed.

We then consider the Newtonian limit of those equations, since this problem is more transparently analyzed in that limit. In the Appendix A we show that the equation of state obtained via the Newtonian limit is an excellent approximation to the one obtained in the general relativistic treatment. Therefore, we use the Newtonian formalism in the rest of the paper, for clarity purpose. In section 3 we use the rotational velocity profile proposed in Persic & Salucci & Stel (1996), PSS profile, to obtain the equation of state and we fixed the free parameters by fitting with them the observed velocities of a set of galaxies. In section 4 we derive the equation of state, starting from the density profile instead. We have used the Pseudo-isothermal density profile (subsection 4.1), the Einasto density profile, Einasto (1965) (subsection 4.2), the Navarro-Frenk-White, NFW, density profile, Navarro & Frenk & White (1997) (subsection 4.3) and the Burkert density profile, Burkert (1995) (subsection 4.4). In section 5 we make a comparison between all the equations of state we have derived for each model and discuss some implications for dark matter detection and possible follow up research.

2 PERFECT FLUID HALO

Although the halo could have been directly considered as a Newtonian system, we used the best available theoretical tool, i.e. general relativity, given the unknown nature of the dark matter, and then test the accuracy of the Newtonian description. We consider a static and spherically symmetric space-time in General Relativity, described by the line element:

$$ds^2 = -e^{2\Phi/c^2} c^2 dt^2 + \frac{dr^2}{1 - \frac{2Gm}{c^2 r}} + r^2(d\theta^2 + \sin^2 \theta d\varphi^2), \quad (1)$$

where the gravitational potential $\Phi(r)$ and the mass function $m(r)$ are functions of the radial coordinate only.

We will take advantage of the fact that one of the geometric potentials can be determined by the observations. Indeed, it can be obtained an expression relating the tangential velocities of test particles, v_t , following stable circular

orbits in this spacetime, with the gravitational potential Φ , by means of solving the geodesic equations for test particles in circular stable orbits (see Matos et al (2000), Matos et al. (2000a), Cabral (2002) and Rahaman et al. (2010) for details on the derivation). Such expression is

$$\frac{\Phi'}{c^2} = \frac{\beta^2}{r}, \quad (2)$$

where $\beta^2 = \frac{v_t^2}{c^2}$.

The same expression, Eq. (2), is obtained in the Newtonian description by simply equating the gravitational force with the centrifugal one for particles in circular orbit.

Thus, given a rotational velocity profile $\beta(r)$, the system of a self-gravitating isotropic fluid in a space time with line element Eq. (1), is left with three unknowns: one geometric, the mass function, and two related to the dark fluid, the pressure and the energy density. The system of equations are two Einstein's equations and the conservation equation, that is, the system is closed. Indeed, using the relation (2), the resulting equations are:

$$n' = 3x^2 \bar{\rho}, \quad (3)$$

$$\left(1 - q \frac{2n}{x}\right) \frac{\beta^2}{x} - q \frac{n}{x^2} = 3qx\bar{p}, \quad (4)$$

$$\bar{p}' + (\bar{p} + \bar{\rho}) \frac{\beta^2}{x} = 0, \quad (5)$$

where prime stands for derivative with respect to x and we have used convenient dimensionless variables n and x for the mass function and the radial distance respectively, such that $m = M_* n$ and $r = R_* x$, where M_* and R_* are the characteristic scales for mass and distance of the system under study. We also define a characteristic density, $\rho_* = M_*/(4/3)\pi R_*^3$, and a characteristic pressure: $p_* = \rho_* c^2$, so that $\rho = \rho_* \bar{\rho}$, and $p = p_* \bar{p}$, with $\bar{\rho}, \bar{p}$ dimensionless functions. In the Eq. 4 it was also introduced the dimensionless parameter $q = M_* G/c^2 R_*$, which measures the characteristic compactness of the system.

Let us consider the Newtonian limit of Eqs. (3-5). Notice that Eq. (3) does not change; in the Newtonian limit it can be considered as the definition of the mass function in terms of the density (see Landau and Lifshitz (1971), and Misner and Sharp (1964)). The second Einstein's equation, in the weak field limit and considering that the pressure is negligible, gives a direct relation between the gravitational potential and the mass function, $\frac{\Phi'}{c^2} = q \frac{n}{x^2}$, hence, in the Newtonian description the two geometric functions are related, in contrast to the general relativity case, where the geometric functions are completely independent functions. Finally, in the conservation equation, the Newtonian limit implies that the pressure is much less than the density, so neglecting the pressure as compared to the density in the second term of Eq. (5), we obtain the usual Euler equation in equilibrium. Thus, the Newtonian limit of the relativistic equations Eqs. (3-5) are:

$$n' = 3x^2 \bar{\rho}, \quad (6)$$

$$\beta^2 x = qn, \quad (7)$$

$$\bar{p}' + \bar{\rho} \frac{\beta^2}{x} = 0. \quad (8)$$

In this way, given the rotational velocity profile, $\beta^2(x)$, the gravitational potential, Φ , and the mass, n , are deter-

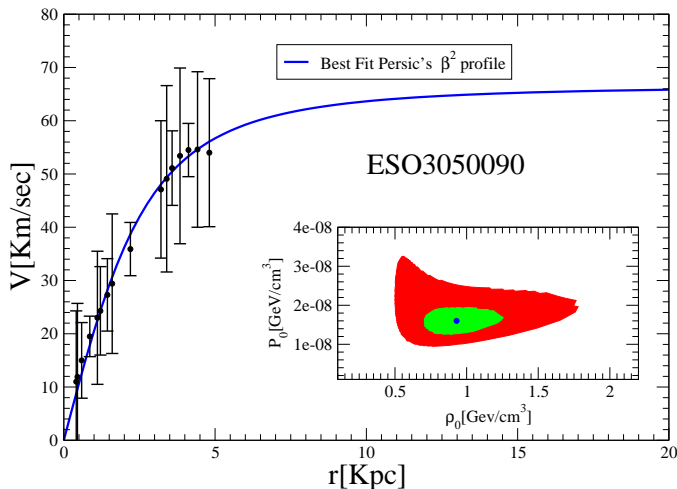


Figure 1. Fit on the rotation curves for the galaxy ESO3050090. Red line corresponds to best fit point as expressed in table 1. Inner figure: Green region corresponds to 68 confidence level and red region to 90% confidence level values for (ρ_0, p_0)

mined directly. Next, the density is determined straightforward, and one has only to solve one differential equation for the pressure, namely:

$$\bar{p}' + \frac{\beta^2}{3q x^3} (\beta^2 x)' = 0. \quad (9)$$

Once the pressure and the density are known, it is possible to determine the equation of state. Notice that $\bar{p} = 0$ is not a solution of Eq. (9) for a given non zero rotational velocity profile. It is mandatory that the dark fluid should have pressure.

In the case when the density profile is the starting point instead of the rotational velocity profile, it is also possible to determine all the functions of the system and again derive an equation of state. We will show examples of both cases in the next section.

The relativistic case is more involved, but an analogous procedure can be followed, and also obtained at the end a differential equation for the pressure, such procedure is detailed in the appendix. We stress the fact that the exact treatment is the relativistic one and we have used it to derive the corresponding equation of state, but we found that the relativistic treatment gives only negligible corrections to the Newtonian results. Thus, from now on we will work only in the Newtonian limit.

Even though the halo could have been directly considered as a Newtonian system, we used the best available theoretical tool, given the unknown nature of the dark matter, and then test the approximated description.

3 DARK MATTER EQUATION OF STATE FROM ROTATIONAL CURVES

There are several profiles which have been proposed to adjust the rotational velocities profiles observed in the galaxies (see, e.g., Courteau 1997).

We will consider the velocity profile proposed by Persic & Salucci & Stel (1996) obtained by adjusting 1023 galaxies which is given by:

$$\beta^2 = \beta_0^2 \frac{x^2}{x^2 + a^2}, \quad (10)$$

where β_0, a are constants. The first one, β_0 , stands for the ratio of the terminal velocity to the speed of light, and a determines how fast the velocity reaches a terminal value. Within the notation of Persic & Salucci & Stel (1996), β_0 is a function of the luminosity of the galaxy. In our present work we will assume that both β_0^2 and a are simply constants that can be fitted to observational data and from now we will refer to Eq. (10) as the PSS rotational velocity profile.

Given $\beta^2(x)$ by Eq. (10), it is straightforward to obtain from Eqs. (6-8) analytical expressions for the mass function, the density and the pressure:

$$n = \frac{\beta_0^2}{q} \frac{x^3}{(x^2 + a^2)} \quad (11)$$

$$\bar{\rho} = \frac{\beta_0^2}{3q} \frac{(x^2 + 3a^2)}{(x^2 + a^2)^2}, \quad (12)$$

$$\bar{p} = \frac{\beta_0^4}{6q} \frac{(x^2 + 2a^2)}{(x^2 + a^2)^2}, \quad (13)$$

and it is then possible to obtain an analytical expression for the equation of state for dark matter:

$$\bar{p} = \frac{\beta_0^4}{48 a^2 q} \left(\frac{12 a^2 q}{\beta_0^2} \bar{\rho} - \left(1 - \sqrt{1 + \frac{24 a^2 q}{\beta_0^2} \bar{\rho}} \right) \right). \quad (14)$$

Furthermore, the density and the pressure profiles as expressed in Eqs. (12,13) allow us to find a relation between β_0^2 and a as functions of the central pressure and the central density $\bar{\rho}_0$ and \bar{p}_0 . Namely

$$a^2 = \frac{3 \bar{p}_0}{q \bar{\rho}_0^2}, \quad \beta_0^2 = \frac{3 \bar{p}_0}{\bar{\rho}_0}. \quad (15)$$

Hence, it is possible to re-write the mass, the density and the pressure for a halo satisfying the PSS's rotational velocity profile, in terms of the central pressure and density. Rewriting the equation of state, Eq.(14), in this way we obtain:

$$\bar{p}(\bar{\rho}) = \bar{p}_0 \left(\frac{3}{4} \left(\frac{\bar{\rho}}{\bar{\rho}_0} \right) - \frac{1}{16} \left(1 - \sqrt{1 + 24 \left(\frac{\bar{\rho}}{\bar{\rho}_0} \right)} \right) \right). \quad (16)$$

Some comments about this equation are in order. The equation of state Eq. (16) reduces to the barotropic equation of state $\bar{p} = \frac{3 \bar{p}_0}{4 \bar{\rho}_0} \bar{\rho}$ in the limit where $\bar{\rho} \ll \bar{\rho}_0$. This has a natural explanation: \bar{p} is a decreasing function, with maximum value \bar{p}_0 at $x = 0$. In the limit $x \rightarrow \infty$ the density decreases and the rotation curve profile tends to a constant value, that is, the behavior of an ideal gas which has a barotropic equation of state.

Eqs. (14) and (16) have two free parameters; either β_0 and a or $\bar{\rho}_0$ and \bar{p}_0 . In order to determine the values of those free parameters and advance with our method, we will use observational data of the rotational curves of several low surface brightness galaxies, reported in de Blok & Bosma (2002). The procedure for a given galaxy, consists in determining the best values of β_0 and a that fits the observed rotational curve through a χ^2 analysis.

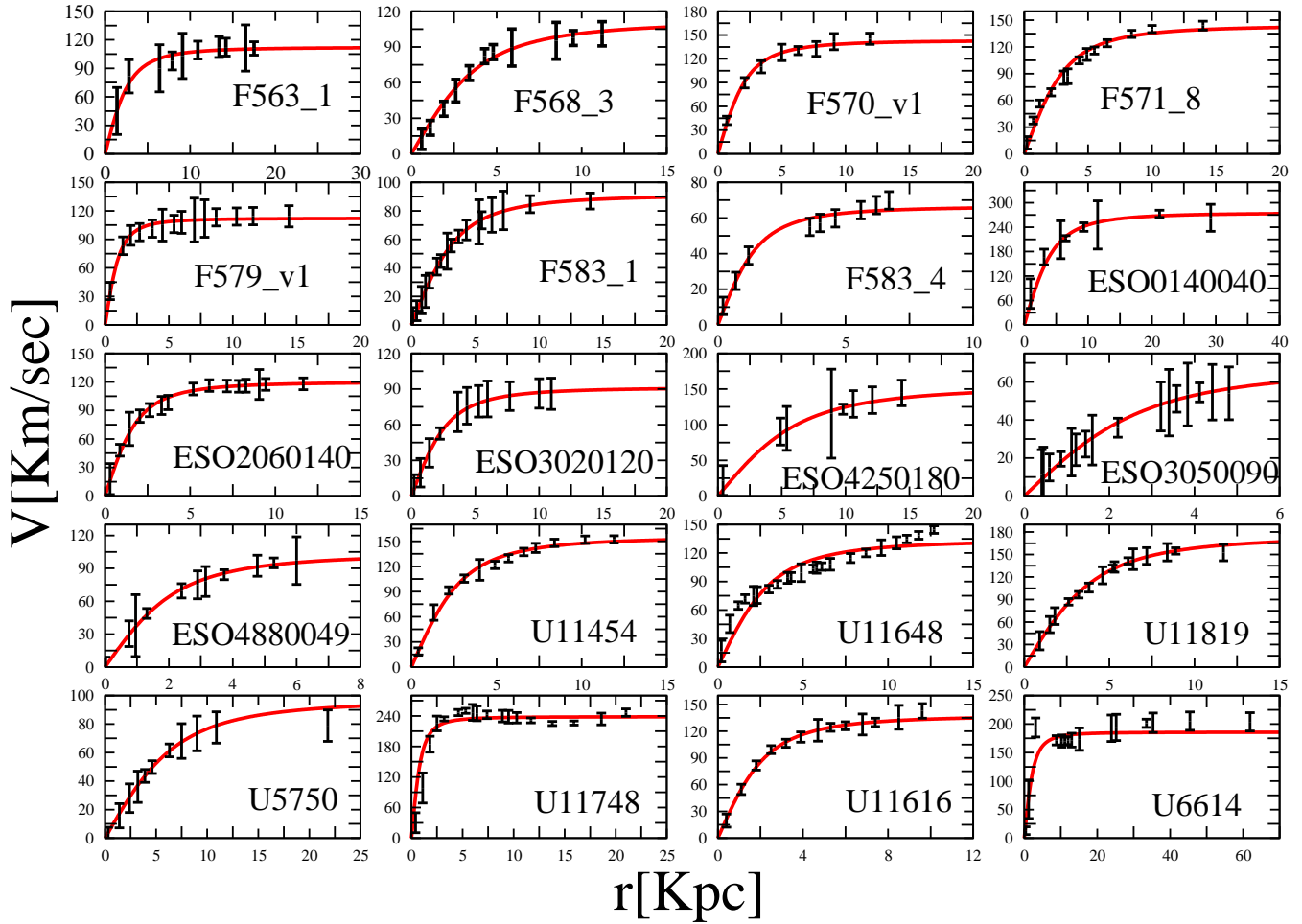


Figure 2. Rotational Curve data from 20 Low Surface Brightness galaxies from de Blok & Bosma (2002). Red lines correspond to the best fit curve using PSS's rotational curve profile.

Let us for instance use the data for the galaxy ESO3050090. The observed rotational velocity as a function of the radial distance from the center of the galaxy is shown in Fig. (1). The best fit points are obtained by minimizing the function

$$\chi^2 = \sum_i \left(\frac{\beta_{theo} - \beta_{exp_i}}{\delta\beta_{exp_i}} \right)^2, \quad (17)$$

where i runs up to the number of points in the data and β_{theo} is computed according to the velocity profile under consideration, i.e. Eq. (10). $\delta\beta_{exp_i}$ is the error in the determination of the rotational velocity.

Note that the terminal velocity is of the order of 100 Km/s, so that, using the Newtonian relation for the mass of the halo: $m(r) = r v_t^2 / G$, taking $G = 4.299 \cdot 10^{-6} \frac{\text{Kpc}(\text{km/s})^2}{M_{\text{Sun}}}$ and the characteristic distance $R_* = 1 \text{ Kpc}$; the characteristic mass of the system is $M_* = 10^{10} M_{\odot}$. With these values of M_* and R_* , we obtain $q = 5 \cdot 10^{-7}$ and the characteristic values of the density and the pressure are: $\rho_* = 1.62 \cdot 10^{-22} \frac{\text{gcm}^{-3}}{\text{cm}^3}$ and $p_* = 1.46 \cdot 10^{-1} \frac{\text{grm}}{\text{cm s}^2}$. We will use these characteristic values from now on.

After the minimization of the χ^2 function we can obtain confidence level regions for the parameters $\bar{\rho}_0$ and \bar{p}_0 which are mapped directly to ρ_0 and p_0 through the characteristic

values ρ_* and p_* . Such regions are shown in the inner panel of Fig. (1). It is shown the allowed region of parameters at 68% (green region) and 90% (red region) confidence level for the central density ρ_0 and central pressure p_0 . Hence, we have a prediction of the central pressure and density for the galaxy obtained from the rotational curve data only.

The same analysis can be performed for any galaxy. For definitiveness we will use the data shown in Fig.(2) taken from Blok & Bosma (2002).

The best fit points for each galaxy are shown in Table (1), either for (a, β_0) or (ρ_0, p_0) . We also present the goodness of the fit, which is given by the ratio of the minimum value of χ^2 over the degrees of freedom, $\chi_{min}^2/\text{d.o.f.}$

The allowed regions for ρ_0 and p_0 at 68% and 90% confidence level obtained for each galaxies are presented in Fig. (3).

The equation of state $\bar{p}(\bar{\rho})$, Eq. (16), gives the functional relation as soon as $\bar{\rho}_0$ and \bar{p}_0 are given. In addition to the allowed regions of the central pressure and density, we have included in Fig. (3) in dashed lines the equations of state $p(\rho)$ that are obtained by evaluating Eq. (16) using the best fit values ρ_0 and p_0 obtained by minimizing the χ^2 using the data of the galaxies U11748 and ESO3050090. As can be seen, most of the allowed regions for (ρ_0, p_0) , and thus, their

| <i>Galaxy</i> | $\beta_0 10^{-4}$ | a | $\rho(0) \frac{\text{GeV}}{\text{cm}^3}$ | $p(0) \frac{\text{GeV}}{\text{cm}^3}$ | $\frac{\chi^2_{\text{min}}}{\text{d.o.f.}}$ |
|---------------|-------------------|------|--|---------------------------------------|---|
| F563 1 | 3.74 | 3.18 | 2.50 | 1.2×10^{-7} | 0.13 |
| F568 3 | 3.71 | 4.53 | 1.22 | 5.6×10^{-8} | 0.34 |
| F570 v1 | 4.78 | 2.55 | 6.40 | 4.9×10^{-7} | 0.35 |
| F571 8 | 4.8 | 3.65 | 3.13 | 2.4×10^{-7} | 2.2 |
| F579 v1 | 3.74 | 1.29 | 15.30 | 7.1×10^{-7} | 0.08 |
| F583 1 | 3.04 | 1.48 | 1.04 | $3. \times 10^{-8}$ | 0.01 |
| F583 4 | 2.22 | 1.77 | 2.85 | 4.7×10^{-8} | 0.57 |
| ESO140040 | 9.2 | 5.08 | 5.91 | 1.7×10^{-6} | 0.45 |
| ESO2060140 | 4.00 | 2.16 | 6.22 | 3.3×10^{-7} | 0.13 |
| ESO3020120 | 3.04 | 3.19 | 1.65 | 5.1×10^{-8} | 0.01 |
| ESO4250180 | 5.12 | 7.19 | 0.92 | 8.1×10^{-8} | 0.12 |
| ESO4880049 | 3.44 | 2.53 | 3.37 | 1.3×10^{-7} | 0.06 |
| ESO3050090 | 2.2 | 3.14 | 0.93 | 1.6×10^{-8} | 0.06 |
| U11454 | 5.18 | 3.32 | 4.42 | 4.0×10^{-7} | 0.81 |
| U11648 | 4.46 | 3.53 | 2.88 | 1.9×10^{-7} | 5.32 |
| U11819 | 5.82 | 4.63 | 2.87 | 3.24×10^{-7} | 0.21 |
| U5750 | 3.23 | 7.75 | 0.31 | 1.1×10^{-8} | 0.01 |
| U11748 | 7.94 | 1.07 | 99.33 | 2.0×10^{-5} | 3.67 |
| U11616 | 4.59 | 2.53 | 5.96 | 4.2×10^{-7} | 0.20 |
| U6614 | 6.19 | 2.85 | 8.54 | 1.1×10^{-6} | 2.35 |

Table 1. Best fit values for (a, β_0) for several low surface brightness galaxies. Those values can be translated into values for the central density and pressure (ρ_0, p_0) . We have taken $R_* = 1$ Kpc, $M_* = 10^{10} M_\odot$, so that $q = 5 \times 10^{-7}$. See below.

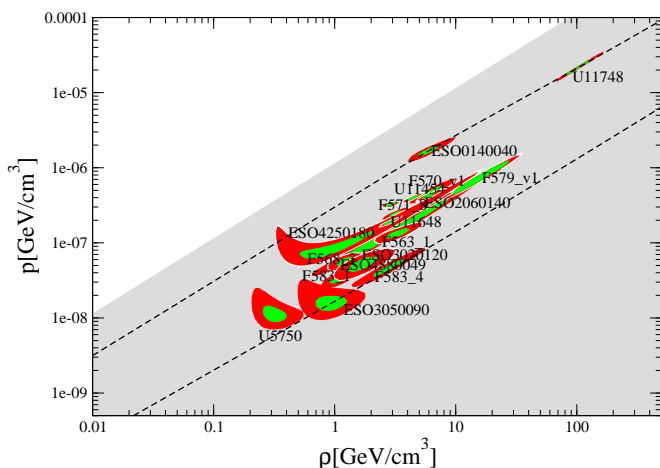


Figure 3. Central density ρ_0 and pressure p_0 for all example galaxies fitted as expressed in Table 1. Green regions corresponds to 68% C.L. and red regions corresponds to 90% C.L. Dashed lines are the evaluation of the dark matter equation of state, Eq. (16) for the best fit point (ρ_0, p_0) for U11748 (upper line) and ESO3050090 (lower line). Grey region is the allowed region obtained with cosmological data obtained by Muller (2005).

corresponding equation of state, for our sample of galaxies are contained between those two dashed lines. In that sense, the velocity profile provides an unique equation of state for all galaxies, where the only free parameters are the central density ρ_0 and central pressure p_0 . From our limited sample of galaxies, we obtain:

$$0.93 \text{ GeV/cm}^3 < \rho_0 < 99 \text{ GeV/cm}^3 \quad \text{and} \\ 1.6 \times 10^{-8} \text{ GeV/cm}^3 < p_0 < 2 \times 10^{-5} \text{ GeV/cm}^3, \quad (18)$$

as allowed intervals.

In the next section we will discuss how much those regions depend on the particular selection of the halo model.

Finally, let us comment about previous bounds on the equation of state obtained by analyzing cosmological observations. In Fig. (3) we have included on gray the limit found in Muller (2005). This limit was obtained assuming a barotropic equation of state for the dark matter $p = \omega_{DM} \rho$. The allowed values for ω_{DM} are $-1.5 \times 10^{-6} < \omega_{DM} < 1.13 \times 10^{-6}$. Similar analysis was done recently, including the latest results from Planck, Xu & Chang (2013), it was obtained that $\omega_{DM} \in 7.07^{+7.46}_{-7.47} \times 10^{-4}$, which is less stringent than the limit obtained by Muller (2005). In contrast, our results imply that if dark matter is modeled as a perfect fluid with a barotropic equation of state, it is not possible to reproduce the rotational curve velocity profiles. However, as can be seen in Fig. (3), the central pressure and densities of all the galaxies we have analyzed are below the limit found in Muller (2005). Hence, we conclude that it could be interesting to repeat the analysis done for the cosmological cases but using the dark matter equation of state Eq. (16) instead that the barotropic relation and to find out if there is consistency at galactic and cosmological scales with an unique equation of state.

4 DARK MATTER EQUATION OF STATE FROM THE MASS DENSITY PROFILE

Our derivation for the equation of state for the dark matter only needs the velocity profile $\beta^2(x)$. For the cases when the mass density profile $\bar{\rho}(x)$ is given, it can be used to determine β . Indeed, given $\bar{\rho}$, the mass function $n(x)$ is computed from Eq. (6) and then, using Eq. (7) $\beta(x)$ is obtained. Furthermore, the other metric coefficient $\Phi(x)$ is computed using Eq. (2) and finally, the pressure $\bar{p}(x)$ is obtained via integration of Eq. (8). In the following we will compute $n(x), \beta^2(x), \Phi(x)$ and $\bar{p}(x)$ for several mass density profiles. Then, the functional relationship $\bar{p}(\bar{\rho})$ will be derived. We will consider the Pseudo-isothermal, Einasto, Navarro-Frenk-White and the Burkert dark matter density profiles.

Note that to perform such procedure in the general relativistic case is more involved. In this case, one obtains a system of equations for Φ' and \bar{p} and, once it is solved, the velocity profile $\beta^2(x)$ is determined by means of Eq. (2). In any case, as it is mentioned above and shown in the appendix, the Newtonian results agree with the relativistic ones to high precision, so that it is enough to consider the Newtonian case.

4.1 Pseudo isothermal mass density profile

An interesting example of a mass density profile which is regular at the origin is given by the pseudo isothermal model, where the dark matter density profile takes the form:

$$\bar{\rho}(x) = \frac{A}{x^2 + x_c^2}, \quad (19)$$

where A and x_c are parameters used to adjust the model to the observations.

In this case, the velocity profile will be given by

$$\beta^2(x) = 3qA \left(1 - \frac{\arctan\left(\frac{x}{x_c}\right)}{\frac{x}{x_c}} \right), \quad (20)$$

and the geometric potentials are, the mass function:

$$n(x) = 3Ax \left(1 - \frac{\arctan\left(\frac{x}{x_c}\right)}{\frac{x}{x_c}} \right), \quad (21)$$

and the gravitational potential

$$\frac{\Phi(x)}{c^2} = 3qA \left(\ln \sqrt{1 + \left(\frac{x}{x_c}\right)^2} + \frac{\arctan\left(\frac{x}{x_c}\right)}{\frac{x}{x_c}} \right). \quad (22)$$

From these expressions, by integration of Eq. (8), one finally obtains the pressure of a pseudo isothermal halo:

$$\bar{p}(x) = \frac{3qA^2}{2x_c^2} \left(\frac{\pi^2}{4} - 2 \frac{\arctan\left(\frac{x}{x_c}\right)}{\frac{x}{x_c}} - \left(\arctan\left(\frac{x}{x_c}\right) \right)^2 \right). \quad (23)$$

In the last expression, we have chosen the integration constant such that the pressure vanishes far from the center of the halo.

Identifying the values of the density and the pressure at the center of the halo, $\bar{\rho}_0$ and \bar{p}_0 , we relate them with the parameters of the model by

$$\bar{\rho}_0 = \frac{A}{x_c^2} \quad \text{and} \quad \bar{p}_0 = \frac{3qA^2}{8x_c^2} (\pi^2 - 8), \quad (24)$$

so that we can write down the previous expressions for the gravitational potential, the mass function, the pressure and the density in terms of the central pressure and the central density. In particular, the gravitational potential can be written as:

$$\frac{\Phi(x)}{c^2} = \frac{8\bar{p}_0}{\bar{\rho}_0(\pi^2 - 8)} \left(\ln \sqrt{2 - \left(\frac{\rho_0}{\bar{\rho}_0}\right)^2} + \frac{\arctan \sqrt{\frac{\bar{\rho}_0}{\rho_0} - 1}}{\sqrt{\frac{\bar{\rho}_0}{\rho_0} - 1}} \right). \quad (25)$$

square root remains always positive.

Finally, the equation of state for the Pseudo-Isothermal density profile in terms of the central parameters is:

$$\bar{p}(\bar{\rho}) = \frac{8\bar{p}_0}{\pi^2 - 8} \times \left[\frac{\pi^2}{8} - \frac{\arctan \sqrt{\frac{\bar{\rho}_0}{\bar{\rho}} - 1}}{\sqrt{\frac{\bar{\rho}_0}{\bar{\rho}} - 1}} - \frac{1}{2} \left(\arctan \sqrt{\frac{\bar{\rho}_0}{\bar{\rho}} - 1} \right)^2 \right]. \quad (26)$$

Although it is not a linear relation between the pressure and the density, when the density is much smaller than the central density $\rho \ll \rho_0$, the equation of state has the limit

$$\bar{p}(\bar{\rho} \ll \bar{\rho}_0) = \frac{4\bar{p}_0}{\bar{\rho}_0 (\pi^2 - 8)} \bar{\rho}, \quad (27)$$

which is a barotropic equation of state, very similar to the equation of state derived in section 3 in the same limiting case.

It is possible to fit the data from the observations of the set of galaxies as done in the previous section.

The pressure as a function of the radial distance $p(x)$ obtained by using either the PSS velocity profile $\beta^2(x)$ or the Pseudo-Isothermal mass density profile $\bar{\rho}(x)$ is regular at $x = 0$. This allows us to rewrite the velocity profile's free parameters in terms of the central density and the central

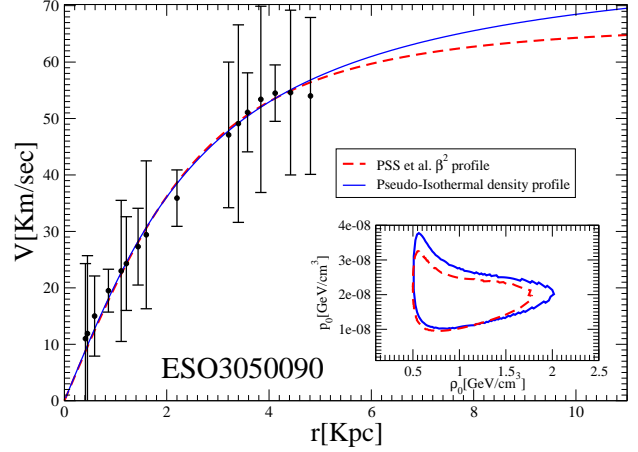


Figure 4. Data points of the rotational velocity for the galaxy ESO3050090 and best fit curve using PSS's velocity profile (dashed line) and velocity profile obtained with the Pseudo-isothermal dark matter density (solid line). Inner figure: Different predictions for the central density and pressure for both velocities profiles

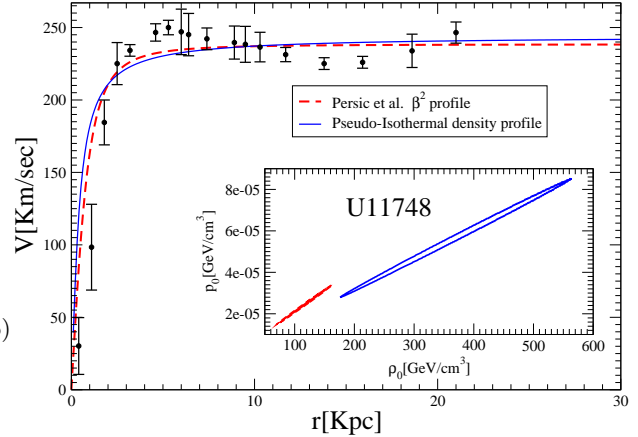


Figure 5. Data points of the rotational velocity for the galaxy U11748 and best fit curve using PSS's velocity profile (dashed line) and velocity profile obtained with the Pseudo-isothermal dark matter density (solid line). Inner figure: Different predictions for the central density and pressure for both velocities profiles

pressure (ρ_0, p_0) with the help of Eq. (24) as done in previous section.

Now we address the question of how much the predictions for ρ_0 and p_0 depend on the election of either the velocity or the mass density profiles, at least for the two profiles we have considered that have regular behavior at $x = 0$. Let us consider again the data for the rotational curve of the galaxy ESO3050090.

As it is shown in Fig. (4), the data can be nicely fitted with either the PSS's velocity profile or the velocity profile derived from the Pseudo-isothermal density profile. The allowed regions for the ρ_0 and p_0 at 90% confidence level are shown in the inner figure. As can be observed, both regions coincide independently of the halo model used. From this figure we may infer that the prediction for the central density and pressure is independent of the parametrization used to fit the rotational curve data.

Nevertheless, the same procedure can be done for the data of the Galaxy U11748. The fits for the rotational velocity data are shown in Fig. (5). Again there is a set of (ρ_0, p_0) that can give a nice fit to the data, but in contrast to the case of the galaxy ESO3050090, the regions for ρ_0 and p_0 obtained in each case are different depending on the functional parametrization of $\beta^2(x)$ that is used. This is shown in the inner figure of Fig. (5) that shows the allowed regions for ρ_0 and p_0 at 90% C.L. for each velocity profile.

A closer look at Fig. (4-5) can help us to understand the reason why in one case it seems that there is a unique determination of the central density and pressure while in other case we found a different determination of the central pressure an density. The data points of the galaxy ESO3050090 exhibit large error bars, hence the allowed values for (ρ_0, p_0) spread over a large region.

On the other hand, the data points for U11748 have smaller error bars and there are more data points that are located for either small or large values of x . The last data points are relevant since the flat behavior of the rotational curve is present. Thus, the fit should consider both regions: the inner region and the flat behavior and the minimization of χ^2 will found a more restricted region for (ρ_0, p_0) that produces a rotational curve consistent with all data points. Hence, we may conclude that the prediction of the central density and pressure will depend on the quality of the velocity profile we are using. It is desirable to have data points with small errors at a wide range of distances from the center of the galaxies.

The determination of the central density has a direct implication in experiments looking for direct or indirect detection of dark matter. From our analysis in the galaxy U11748 we have found that the determination of the central density strongly depends on the density or velocity profile we are using. We will discuss more about this point in section 5.

We end this sub-section by presenting the corresponding results for the isothermal sphere. In this case, the density profile is given by

$$\bar{\rho}_{\text{Iso}}(x) = \frac{A}{x^2}, \quad (28)$$

and it is straightforward to determine the corresponding mass, velocity profile and the pressure, from Eqs. (6-8):

$$\bar{n}_{\text{Iso}}(x) = 3Ax, \quad (29)$$

$$\Phi'_{\text{Iso}}(x)/c^2 = 3q \frac{A}{x}, \quad (30)$$

$$\beta^2_{\text{Iso}}(x) = 3qA, \quad (31)$$

$$\bar{p}_{\text{Iso}}(x) = \frac{3qA^2}{2x^2}, \quad (32)$$

where we have set to zero the integration constant in the pressure. In this way, we obtain that the equation of state for the isothermal dark fluid sphere is

$$\bar{p}_{\text{Iso}} = \frac{3qA}{2} \bar{\rho}_{\text{Iso}}. \quad (33)$$

It is a barotropic equation of state and actually coincides, as it should, with the limit of the equation of state for the pseudo isothermal halo far from the central region, Eq. (27) when $\bar{p}_0, \bar{\rho}_0$ are rewritten in terms of the original parameters Eq. (24).

In this case, $\beta^2_{\text{Iso}}(x)$ is a constant, and could play the role of a measure of an analogous to the temperature of the dark halo. However, it is impossible to fit the rotational velocity curve in this case and then, a isothermal equation of state can not describe the dark matter if it is desired a good fit with the rotational velocity when dark matter is treated as a perfect fluid.

Nevertheless, in the regions where the rotational velocity profile is constant, the isothermal sphere can give some hints on the dark matter properties.

4.2 Einasto's density profile

The derivation of the equation of state can be performed for any given rotational velocity profile or density profile proposed. Previously we have shown profiles from which the behavior of both the density and the pressure at the center are regular.

Nevertheless, there are many other dark matter density profiles. Among them, a three parametric function for the density profile was proposed by Einasto (1965) several years ago and has recently received more attention. It is given by

$$\rho_{\text{Ein}} = \rho_0 e^{-\frac{2}{L} \left(\left(\frac{x}{x_c} \right)^L - 1 \right)}, \quad (34)$$

where ρ_0, x_c and L are free parameters. This case is also regular at the origin, $\rho(x=0) = \rho_0 e^{\frac{2}{L}}$, for finite ρ_0, L , although it can be very cuspy for small values of the parameter L .

It is possible to obtain an analytic expression for the velocity profile by integration of Eq. (6) and with the help of Eq. (7) (obtained through Maple16):

$$\begin{aligned} \beta^2_{\text{Ein}} = & \frac{q \rho_0 L^{\frac{3(L+1)}{L}} x^2 e^{-\frac{2}{L} \left(\frac{x}{x_c} \right)^L - 2}}{4 \left(8 \left(\frac{1}{L} \right) \right) \left(\frac{x}{x_c} \right)^{\frac{L+3}{2}} (L+3) (2L+3)} \times \\ & \left(L \left(2^{\frac{3(1+L)}{2L}} + 2^{\frac{3+L}{2L}} \left(\frac{x}{x_c} \right)^{-L} (L+3) \right) \times \right. \\ & \text{WhittakerM} \left(-\frac{L-3}{2L}, \frac{2L+3}{2L}, \frac{2}{L} \left(\frac{x}{x_c} \right)^L \right) + \\ & \left. 2^{\frac{3+L}{2L}} \left(\frac{x}{x_c} \right)^{-L} (L^2 + 6L + 9) \times \right. \\ & \left. \text{WhittakerM} \left(\frac{L+3}{2L}, \frac{2L+3}{2L}, \frac{2}{L} \left(\frac{x}{x_c} \right)^L \right) \right). \end{aligned} \quad (35)$$

Using Eq. (35) it is possible to fit our set of velocities profiles. In Fig. (6) we give a couple of examples. Those galaxies where only data points for small values of the distance to the center of the galaxies are given can be easily fitted by the Einasto profile (for instance ESO3050090). But for those galaxies that start to show the characteristic flat behavior for large values of x , it is more difficult to have a good fit. This behavior can be explained through Eq. (35) since $\lim_{x \rightarrow \infty} \beta(x)_{\text{Ein}} = 0$. In other words, Einasto's profile can not have an extremely large flat behavior for the rotational curves.

The mass function and the gradient of the gravitational potential are directly obtained from the velocity profile: $n_{\text{Ein}} = \frac{x}{q} \beta^2_{\text{Ein}}$, and $\Phi'_{\text{Ein}}/c^2 = \frac{\beta^2_{\text{Ein}}}{x}$. Then, we can obtain the pressure by integration of Eq. (8). We did not find

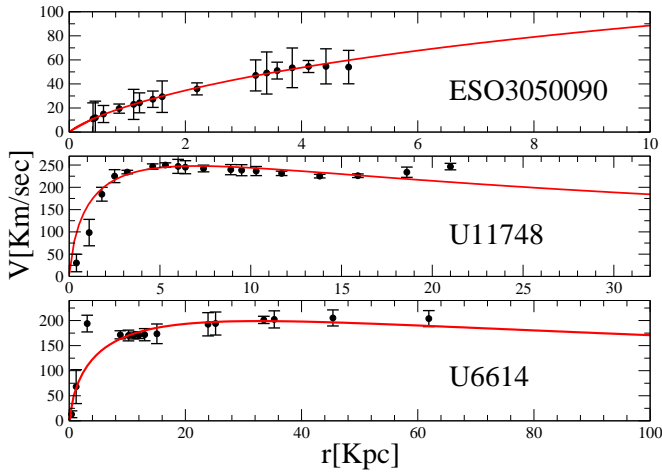


Figure 6. Fit for some LSB galaxies by using the Einasto's velocity profile Eq. (35)

analytical expression, but this can be done numerically. In Fig. (7) we show the equation of state obtained with the best fit parameters for the galaxy U11748.

Due to the form of $\beta(x)_{Ein}$ for large values of x , contrary to the PSS's velocity profile and the Pseudo-isothermal density profile that show a barotropic equation of state for small values of the density, the Einasto's equation of state have a different behavior. For instance, using the best fit values obtained with the data points of the galaxy U11748, the resulting equation of state have a polytropic behavior for small values of the density (in the limit $\rho \ll \rho_0$). That is, when $x \rightarrow \infty$ the Einasto equation of state behaves as $p \sim \rho^\gamma$ with $\gamma \simeq 1.23$. (see Fig. (7)).

We will end this sub-section by comparing the Einasto equation of state with another polytropic equation that arise when dark matter is assumed to be a free gas of fermions at zero temperature. In the case when the equation of state is given, the study of an equilibrium configuration is described by the Tolman-Oppenheimer-Volkov, TOV, equations Tolman (1939), Oppenheimer and Volkov (1939), see also Silbar and Reddy (2004). Notice that this is not the case described in the present work, as long as we derive the equation of state from the observations.

Indeed, the equation of state for non interacting fermions can be directly computed (see Narain et al. (2006) for instance):

$$\begin{aligned} \rho &= \frac{1}{\pi^2} \int_0^{k_F} k^2 \sqrt{m_F^2 + k^2} dk \\ &= \frac{m_f^4}{8\pi^2} \left((2z^3 + z)(1 + z^2)^{1/2} - \sinh^{-1}(z) \right), \end{aligned} \quad (36)$$

$$\begin{aligned} p &= \frac{1}{3\pi^2} \int_0^{k_F} \frac{k^4}{\sqrt{m_F^2 + k^2}} \\ &= \frac{m_f^4}{24\pi^2} \left((2z^3 - 3z)(1 + z^2)^{1/2} + 3 \sinh^{-1}(z) \right), \end{aligned} \quad (37)$$

with $z = k_F/m_f$, k_F the Fermi momentum and m_F the mass of the hypothetical fermion that will represent the dark matter particle.

Eqs. (37) are in units where $\hbar = c = 1$. The only free parameter is the mass of the hypothetical dark fermion m_F .

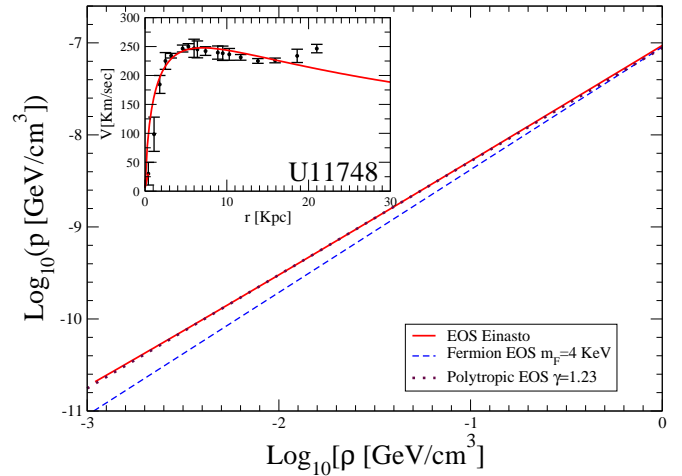


Figure 7. Equation of state obtained using the Einasto's density profile. Dashed line shows the equation of state for a fermion with mass of 4 KeV.

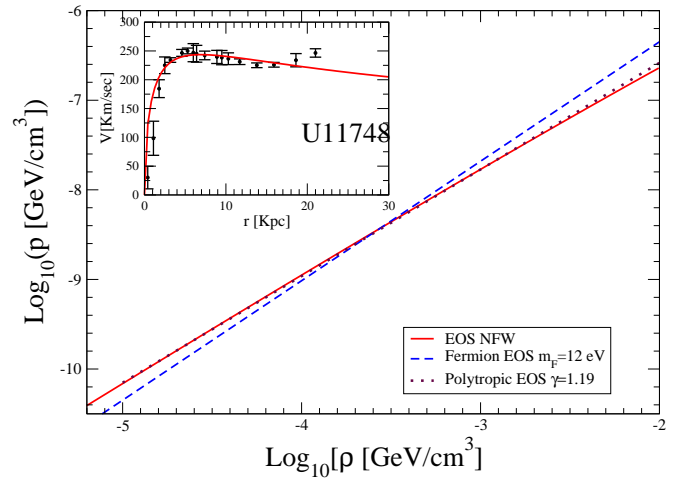


Figure 8. Equation of state obtained using the NFW's density profile. Dashed line shows the equation of state for a fermion with mass of 4 KeV. Dotted line corresponds to a polytropic fit with $\gamma = 1.19$

In Fig. (7) in addition to the equation of state obtained by using the Einasto density profile we have added the resulting equation of state for a free fermion at zero temperature given by Eqs. (37) for a fermion mass of $m_F = 4$ KeV. This comparison might suggest that the equation of state obtained by fitting either the rotational curve profiles or the dark matter density profile will not be mimicked by the equation of state of a free fermion at zero temperature. In the low energy limit, the fermion has a polytropic equation of state with $\gamma = 5/3$, which is a little bit far from the index for the Einasto profile, or the PSS's velocity profile or the pseudo-isothermal, the last two have a barotropic equation of state in the low energy limit.

4.3 Navarro-Frenk-White mass density profile

Numerical simulations in the frame of the Λ -Cold Dark Matter paradigm predicts a cuspy dark matter profile named the Navarro-Frenk-White mass density profile (NFW):

$$\bar{\rho} = \frac{\bar{\rho}_0}{x(x+x_c)^2}. \quad (38)$$

As done in the previous section, it is straightforward to obtain the mass function, the velocity profile, and the gravitational potential from the NFW density profile, namely:

$$n(x)_{\text{NFW}} = 3\bar{\rho}_0 \left(\ln \left(1 + \frac{x}{x_c} \right) - \frac{x}{x+x_c} \right) \quad (39)$$

$$\beta^2(x)_{\text{NFW}} = \frac{3q\bar{\rho}_0}{x} \left(\ln \left(1 + \frac{x}{x_c} \right) - \frac{x}{x+x_c} \right), \quad (40)$$

$$\Phi(x)_{\text{NFW}/c^2} = -\frac{3q\bar{\rho}_0}{x} \ln \left(1 + \frac{x}{x_c} \right), \quad (41)$$

where the integration constant in the mass function, n , has been chosen such that $n(0) = 0$.

With these expressions, it is possible to obtain the pressure for the NFW which is given by:

$$\begin{aligned} \bar{p}(x)_{\text{NFW}} = & \frac{3q\rho_0^2}{2x_c^4} \left[3 \ln \left(1 + \frac{x}{x_c} \right)^2 - \ln \left(\frac{x}{x_c} \right) + \right. \\ & \frac{x^3 - 5x_c x^2 - 3x_c^2 x + x_c^3}{x^2(x+x_c)} \ln \left(1 + \frac{x}{x_c} \right) + \\ & + 6 \operatorname{dilog} \left(1 + \frac{x}{x_c} \right) - \ln \left(\frac{x}{x_c} \right) + \pi^2 + \\ & \left. - \frac{x_c(7x^2 + 9x_c x + x_c^2)}{x(x+x_c)^2} \right], \quad (42) \end{aligned}$$

where $\operatorname{dilog}(x) = \int_1^x \frac{\ln(t)}{1-t} dt$ is the dilogarithm function, and

we have chosen the integration constant such that the pressure vanishes at infinity. It can be seen that the pressure at $x = 0$ is not defined, hence, it is not possible to relate the free parameter x_c with the central pressure.

Nevertheless, with the help of Eq. (40) we can fit the rotational curves data by varying ρ_0 and x_c and evaluate the density and the pressure for NFW and derive the corresponding equation of state. A numerical evaluation of the resulting equation of state is shown in Fig. (8).

The NFW profile implies, as the Einasto profile, a velocity profile that can not reproduce flat rotation curves for large values of the radial distance. As can be seen from Eq. (40), the velocity tends to zero in the limit $x \rightarrow \infty$. In the same way, the resulting equation of state will not present the barotropic behavior for small values of the density. As can be seen in Fig. (8), the NFW profile produces a polytropic equation of state with a value of $\gamma \simeq 1.19$, which differs to the Einasto's case. For completeness we have also plotted the equation of state for a non interacting fermion, as we did for the Einasto profile. In both cases we have used the best fit point for x_c, ρ_0 obtained from the fit to the galaxy U11748. Similar plots are obtained for other galaxies from our sample listed in Table (1).

We end this sub-section by mentioning that an study along these lines was performed by Matos & Núñez & Sussman (2004), working in a Post-Newtonian description of the NFW dark halo. An equation of state for the dark fluid was proposed, not derived as it is done in this work, considering

a polytropic relation between the pressure and the density, which now we see, it was a good guess.

4.4 Burkert mass density profile

Finally, another interesting density dark matter profile was proposed by Burkert (1995).

$$\rho_{\text{Burkert}} = \frac{\rho_0}{\left(1 + \frac{x}{x_c}\right) \left(1 + \left(\frac{x}{x_c}\right)^2\right)} \quad (43)$$

As done in previous subsections, it is possible to obtain the mass function, the velocity profile and the gravitational potential for the NFW density profile, namely:

$$\begin{aligned} n_{\text{B}}(x) = & \frac{3\rho_0 x_c^3}{2} \left[\frac{1}{2} \ln \left(\left(1 + \frac{x}{x_c} \right)^2 \left(1 + \left(\frac{x}{x_c} \right)^2 \right) \right) + \right. \\ & \left. - \tan^{-1} \left(\frac{x}{x_c} \right) \right] \quad (44) \end{aligned}$$

$$\begin{aligned} \beta^2_{\text{B}} = & \frac{3q\rho_0 x_c^3}{2x} \left[\frac{1}{2} \ln \left(\left(1 + \frac{x}{x_c} \right)^2 \left(1 + \left(\frac{x}{x_c} \right)^2 \right) \right) + \right. \\ & \left. - \tan^{-1} \left(\frac{x}{x_c} \right) \right] \quad (45) \end{aligned}$$

$$\begin{aligned} \frac{\Phi_{\text{B}}}{c^2} = & -\frac{3q\rho_0 x_c^2}{4x} \left[- (x - x_c) \ln \left(1 + \left(\frac{x}{x_c} \right)^2 \right) + \right. \\ & \left. + 2(x + x_c) \left(\ln \left(1 + \frac{x}{x_c} \right) - \tan^{-1} \left(\frac{x}{x_c} \right) \right) \right]. \quad (46) \end{aligned}$$

The pressure can be computed and an analytical expression can be found, with Wolfram's Mathematica, however it is quite long and not enlightening, so we do not write it down, but use it for the numerical evaluations.

Note that $\lim_{x \rightarrow \infty} \beta(x) = 0$, and although the decay of the rotational curve can be very small, at the end it is not possible to have flat rotation curves for extremely large values of x . Furthermore, for low densities $\rho \ll \rho_0$, the resulting equation of state also has a polytropic behavior $p \sim \rho^\gamma$, very similar to the NFW profile, i.e. $\gamma = 1.19$.

5 DISCUSSION

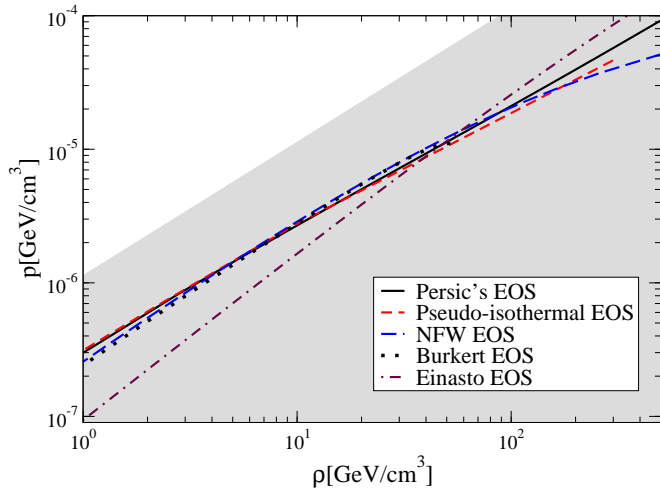
The most direct evidence at galactic scale of the existence of dark matter comes from the rotational curves of galaxies. We have shown that by modeling the dark matter as a perfect fluid, it is possible, using only the data coming from the rotational curves, to obtain the density and pressure of dark matter fluid, and the two metric functions (the mass and the gravitational potential). In particular, the velocity profile proposed by Persic & Salucci & Stel (1996) and the Pseudo-isothermal dark matter density profile are two examples where all those functions are regular at the center of the galaxy. Even more, in some cases, an analytical functional relation of the pressure as a function of the density $p(\rho)$, that is, the equation of state for the dark matter, can be derived.

The free parameters in the equation of state are fixed by fitting the observed rotational curve velocities with the velocity derived from each dark matter profile.

In Table (2) we have summarized the behavior and some

Table 2. Behavior of the density $\rho(x)$, pressure $p(x)$ and rotational velocity $\beta(x)$ for different halo models at values of interest of the radial coordinate x .

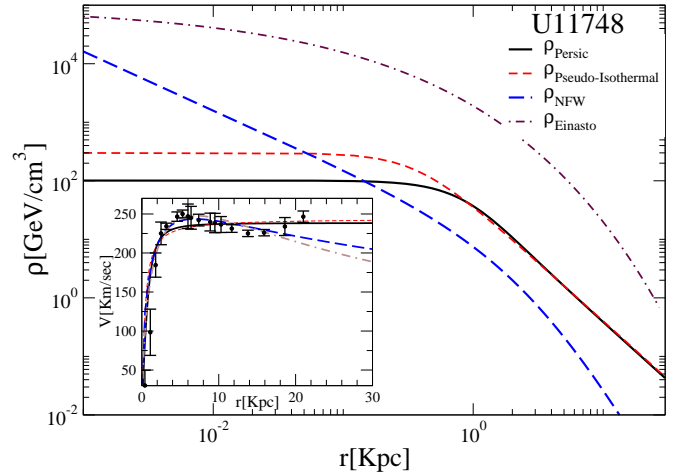
| | Behavior $\rho(x=0)$ | Behavior $p(x=0)$ | $\lim_{x \rightarrow \infty} \beta(x) = v_\infty/c$? | Behavior $P(\rho \ll 1)$? |
|------------------------------|----------------------|-------------------|---|-------------------------------------|
| PSS's $\beta(x)$ profile | Regular | Regular | Yes | Barotropic |
| Pseudo-isothermal DM profile | Regular | Regular | Yes | Barotropic |
| Einasto DM profile | Regular | Not defined | No | Polytropic ($\gamma \simeq 5/4$) |
| NFW DM profile | Not defined | Not defined | No | Polytropic ($\gamma \simeq 1.19$) |
| Burkert DM profile | Regular | Not defined | No | Polytropic ($\gamma \simeq 1.19$) |

**Figure 9.** All equations of state for the best fit parameter for the galaxy U11748.

of the properties of the density, the pressure and the velocity profile for the different halo models at two values of the radial coordinate. Furthermore, the behavior of the equation of state for very low values of the density is also described for the velocity profile for all dark matter density profiles used in this work. We want to stress that, contrary to other approaches, where an equation of state for the dark matter fluid has been proposed, here we have derived such function by using the data from the rotational curves of a set of low surface brightness galaxies. The resulting equation of state is neither barotropic or polytropic near the central part of the galaxy, as usually assumed, and we may conclude that a barotropic equation of state can not fit the observed rotational curves of the galaxies.

Since both the pressure $p(x)$ and dark matter density profiles in the PSS's and Pseudo-isothermal profiles are regular at the origin, it is possible to related the central pressure p_0 and density ρ_0 with the only two free parameters of $\beta(x)$. This is important because allows us to understand that the equation of state has a functional dependence universal for all galaxies, and the free parameters, that is, the central pressure and density are related with the evolution history of the galaxy. Moreover, those equation of state has a barotropic limit for $\rho \ll \rho_0$ and flat rotation curves for large values of the radial coordinate.

Another interesting point, is that even if the dark matter density profile is regular at the origin, it does not imply that the pressure will be regular. See for instance the Burkert

**Figure 10.** Density profiles for the galaxy U11748 with the best fit points. Observe the difference in the determination of the local dark matter density

and Einasto density profiles that has regular density but an ill-defined pressure at the center of the galaxy. Furthermore, the Einasto, Burkert and Navarro Frenk White density profiles can not produce flat rotational curves for large values of the radial coordinate, and the resulting equation of state for low values of the density ($\rho \ll \rho_0$) have a polytropic equation of state $p(\rho) \sim \rho^\gamma$ with γ given in Table (2).

We show in Fig. (9) the equations of state obtained for all dark matter and velocity profiles mentioned above. For definitiveness we have selected the galaxy U11748 and fitted the free parameters of each profile with its rotational velocities data. Although any other galaxy can be used with similar results. As can be seen, there is a region where almost all equation of state superpose, and there are differences either for very low or very high densities. That is, in order to discriminate which equation of state is the most appropriate to describe dark matter, it will be necessary to study what characteristic compact objects produce the specific equation of state (i.e. the high density regime) or to study the ultra low density regime (i.e. the intergalactic medium).

In the same manner as the behavior of the resulting equation of state in the high density regime depends on the dark matter density profile adopted, all other functions depend on the profile used. This may have implications for the indirect detection of dark matter. See for instance Fig. (10), where we have plotted the density as a function of the radial coordinate using the best fit values of our particular example of the U11748 galaxy. As can be noted, the prediction for

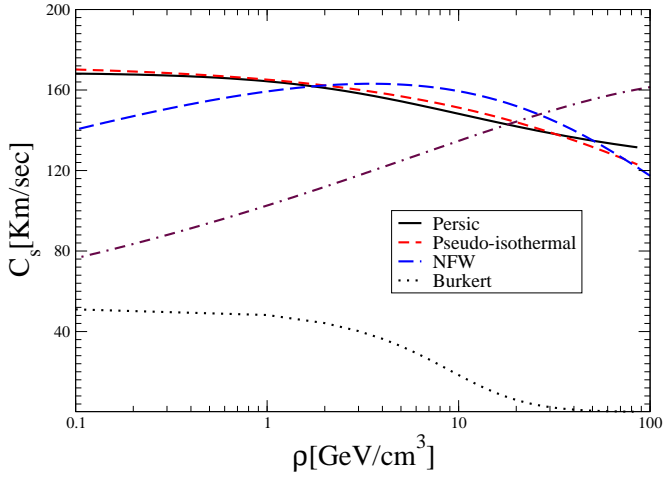


Figure 11. The sound speed for the Dark matter fluid for different dark matter profiles. For definitiveness we have used the best fit points of the galaxy U11748.

the density may change in orders of magnitude. Specially at the center of the galaxy. Indirect detection of dark matter depends strongly on the amount of dark matter at the center of the galaxy, hence the prediction may change drastically depending on the dark matter density profile used.

Another quantity that may differ drastically depending on the profile used is the *Sound Speed* of the fluid. Indeed, it is straightforward to compute the sound speed of the dark matter fluid $C_s^2 = \partial P / \partial \rho$. For the PSS's and Pseudo-isothermal profiles, analytical expressions can be obtained. For the PSS's velocity profile:

$$C_s^2 = \frac{3p_0}{4\rho_0} \left(1 + \left(1 + 24 \frac{\rho}{\rho_0} \right)^{-1/2} \right), \quad (47)$$

while for the Pseudo-isothermal profile

$$C_s^2 = \frac{4p_0}{(\pi^2 - 8)(\rho_0 - \rho)} \left(1 - \frac{\tan^{-1} \sqrt{\frac{\rho_0}{\rho} - 1}}{\sqrt{\frac{\rho_0}{\rho} - 1}} \right) \quad (48)$$

The NFW, Einasto and Burkert sound speed can be obtained by numerical derivation of the corresponding equation of state. As can be see in Fig. (11), the behaviors are very different, some of them change drastically as a function of the density.

This work was supported in part by DGAPA-UNAM grants IN115311, and IN103514, as well as a SNI-México grant and Conacyt 167335.

APPENDIX A: GENERAL RELATIVISTIC DESCRIPTION

From the general relativistic equations, Eqs. (3-5), it can be obtained an equation (with no approximations) for the mass function as the only free function, as was done in Núñez et al. (2010). In this case, however, we are more interested in the dark fluid properties, and, after some manipulation of these equations, we obtain an equation involving only the pressure, \bar{p} :

$$\bar{p}' + S(x) \bar{p} = T(x), \quad (A1)$$

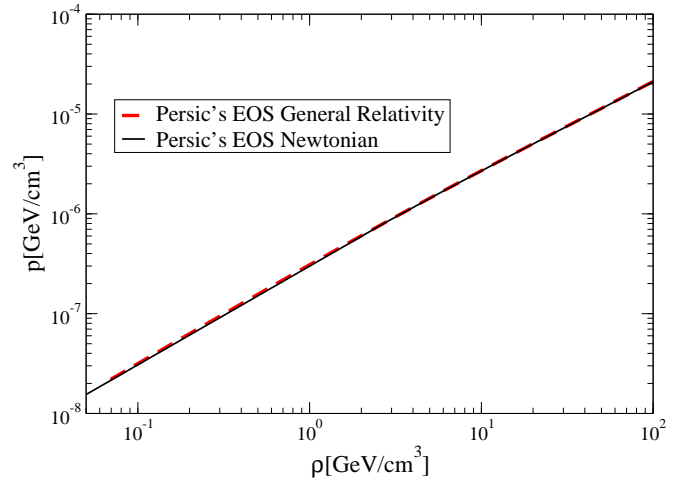


Figure A1. Comparison of the resulting equation of state for the data points of the the galaxy U11748, the PSS's rotational velocity profile

with

$$S(x) = - \frac{2\beta^2 (1 + \beta^2 - 2\beta^4 - x\beta^{2'})}{(1 + \beta^2)(1 + 2\beta^2)x},$$

$$T(x) = - \frac{\beta^2 (\beta^2 + 2\beta^4 + x\beta^{2'})}{3(1 + \beta^2)(1 + 2\beta^2)x^3 q}. \quad (A2)$$

It is the generalization of Eq. (9) to the general relativistic case. The solution for the pressure, expressed in terms of the observed rotational velocity profile, $\beta(x)$, has the form

$$\bar{p} = \frac{\int e^{\int^x S(x') dx'} T(x) dx + C}{e^{\int^x S(x') dx'}}. \quad (A3)$$

where the value of the integration constant, C , is set by the appropriate boundary conditions.

The density and the mass of the dark perfect fluid can be directly computed from Eqs. (3-4), once the pressure is determined:

$$\bar{\rho} = \frac{\beta^2 + 2\beta^4 + x\beta^{2'}}{3(1 + 3\beta^2 + \beta^4)x^2 q} - \frac{3 + 5\beta^2 - 2\beta^4 - 2x\beta^{2'}}{(1 + 3\beta^2 + \beta^4)} p, \quad (A4)$$

and

$$n = \frac{\beta^2}{(1 + 2\beta^2)q} x - 3 \frac{x^3}{(1 + 2\beta^2)} p. \quad (A5)$$

This is the exact treatment, the general relativistic one, to deal with the dark perfect fluid. it provides the means to asses the accuracy of the Newtonian description. We also solved the cases presented in this work within this exact treatment, and the results have an excellent agreement with the Newtonian ones, so that one can use such results with confidence.

In order to see the accuracy of the Newtonian treatment developed in all the article, we present a comparison the General Relativistic results vs the Newtonian result for our well worked U11748 galaxy. See Fig. (A1)

REFERENCES

Avelino A., Cruz N., Nucamendi U., 2012, arXiv 1211.4633.

- Binney J., Tremaine S., 2010, Galactic Dynamics. Princeton Series in Astrophysics. Princeton University Press, second edition.
- Bertone G., Hooper D., Silk J., 2005, Phys. Rept. 405, 279. arXiv hep-ph/0404175.
- Blok de W. J. G., Bosma A., 2002, Astron.Astrophys. 385, 816. arXiv astro-ph/0201276.
- Burkert A., 1995, Astrophys.J. Lett. 447, L25.
- Cabral-Rosetti L. G., Núñez D., Sussman R. A., Matos T., 2002, Rev. Mex. Fis. 49S2, 91. arXiv hep-ph/0206082.
- Calabrese E., Migliaccio M., Pagano L. et al, 2009, Phys. Rev. D80, 063539.
- Carrick J. D., Cooperstock F. I., 2012, Astrophys. Space Sci., 337, 321.
- Cooperstock F. I., Tieu S., 2005a, astro-ph/0507619
- Cooperstock F. I., Tieu S., 2005b, astro-ph/0512048
- Cooperstock F. I., Tieu S., 2006, Mod. Phys. Lett. A, 21, 2133
- Cooperstock F. I., Tieu S., 2007, Int. J. Mod. Phys. A, 22, 2293
- Cooperstock F. I., Tieu S., 2008, Mod. Phys. Lett. A, 23, 1745
- Cooperstock F. I., Tieu S., 2005, astro-ph/0507619.
- Courteau S., 1997, Astrophys.J. 114, 2402.
- Dodelson S., 2010, Modern Cosmology. Academic Press.
- Einasto J., 1965, Trudy Inst. Astrofiz. Alma-Ata, 5, 87.
- Faber T., Visser M., 2006, MNRAS, 372, 136. arXiv astro-ph/0512213.
- Gaitskell R.J., 2004, Ann.Rev.Nucl.Part.Sci. 54 315
- Guzmán F. S., Lora-Clavijo F. D., 2011, MNRAS, 415, 225. arXiv 1103.5497.
- Landau L. D., Lifshitz E. M., 1971, The Classical Theory of Fields (Volume 2 of A Course of Theoretical Physics) Pergamon Press.
- Matos, T., Guzmán F. S., Núñez D., 2000, Phys. Rev. D62, 061301. arXiv astro-ph/0003398.
- Matos, T., Núñez D., Guzmán F. S., Ramírez, E., 2000, Gen. Rel. Grav. 34, 283. arXiv astro-ph/0005528.
- Matos, T., Núñez D., Sussman R., 2005, Gen. Rel. and Grav. 37, 769.
- Misner, Ch. W., Sharp, D. H., 1964, Phys. Rev. 136. B571.
- Müller Ch. M., 2005, Phys. Rev. D71, 047302. arXiv astro-ph/0410621.
- Narain G., Schaffner-Bielich J., Mishustin I. N., 2006, Phys. Rev. D74, 063003
- Navarro J. F., Frenk C. S., Withe D. M. S., (1997) Astrophys. J. 490, 493.
- Núñez D., Gonzalez-Morales A. X., Cervantes-Cota J. L., Matos, T., 2010, Phys. Rev. D82, 024025. arXiv 1006.4875.
- Pepe C., Pellizza L. J., Romero G. E., 2011, MNRAS, 420, 3298.
- Persic M., Salucci P., Stel F., 1996, MNRAS, 281, 27. arXiv astro-ph/9506004.
- Rahaman F., Nandi K.K., Bhadra A., Kalam M., Chakraborty K., 2010, Phys.Lett. B694 10-15
- Serra A. L., Romero M., 2011, arXiv gr-qc/1103.5465.
- Silbar R. R. and Reddy S., 2004, Am. J. Phys. **72** 892
- Smith P.F., Lewin J.D., 1990, Phys. Rept. 187, 203.
- Tolman R. C. , 1939, Phys. Rev. 55, 364373
- Oppenheimer J. R. and Volkov G. M. , 1939, Phys. Rev. 55, 374381.
- Xu L., Chang Y., 2013, Phys. Rev. D88, 127301.